Hydrol. Earth Syst. Sci. Discuss., 6, 5243–5278, 2009
www.hydrol-earth-syst-sci-discuss.net/6/5243/2009/

Hydrology and Earth System Sciences Discussions

Papers published in *Hydrology and Earth System Sciences Discussions* are under open-access review for the journal *Hydrology and Earth System Sciences*

A regional model to predict the distribution patterns of alpine permafrost in the western part of the Qilianshan Mountains, on the northeastern edge of the Qinghai-Tibetan Plateau

Y. Sheng[1], J. Li[1], J. Wu[1], B. Ye[2], and J. Wang[2]

[1]State Key Laboratory of Frozen Soil Engineering, Cold and Arid Regions Environmental and Engineering Research Institute, Chinese Academy of Sciences, Lanzhou 730000, China
[2]State Key Laboratory of Cryospheric Science, State Key Laboratory of Cryospheric Science, Chinese Academy of Sciences, Lanzhou 730000, China

Received: 23 May 2009 – Accepted: 16 June 2009 – Published: 4 August 2009

Correspondence to: Y. Sheng (sheng@lzb.ac.cn)

Published by Copernicus Publications on behalf of the European Geosciences Union.

Abstract

A field investigation and measurement of ground temperatures in boreholes was carried out in the upper area of Shule River in the western part of the Qilianshan Mountains, in the northeast of the Qinghai-Tibetan Plateau in 2008. On the basis of this a sketchy distribution pattern of permafrost in this area was established. A regional permafrost model considering the effects of latitude, altitude, slope and aspect on distribution of permafrost was developed. The effect of latitude was calculated by the Gauss curve as proposed by Cheng, and then added to the effect of altitude. A linear relationship was found between altitude and the measured ground temperatures. For the effects of slope and aspect which mainly affected the amount and spatial distribution of the incoming solar radiation, a linear equation based on increments of the incoming solar radiation and the changes in ground temperature was used to evaluate their influence on the development of permafrost. A distribution map of the frozen ground, as well as a classification map of permafrost based on ground temperatures was produced using the ARCGIS software. In addition, the spatial distribution patterns of frozen ground and each permafrost type in this region were also analyzed.

1 Introduction

In China, permafrost is widely distributed in the high latitude area of the northeastern Region and in the mid-low latitude and high-altitude area of the Western mountains regions. The former is known as high-latitude permafrost and the latter as high-altitude permafrost (Zhou et al., 2000). Compared with the high-latitude permafrost, the high-altitude permafrost has the characteristics of higher ground temperatures, shallower depth of active layers beneath the surface, weaker stability, and widespread distribution (Jin et al., 2006). Hence, they are more sensitive to global climate changes. With the social and economic development in mountainous areas, the distribution patterns and characteristics of alpine permafrost are urgently required for the building and

HESSD

6, 5243–5278, 2009

maintenance of various engineering constructions.

Since the 1990s, the study of the distribution patterns of permafrost in mountains and high altitudes has been an important topic in alpine permafrost art, and was dealt with closely at two international conferences on permafrost. At the seventh International Conference on Permafrost in Yellowknife, Canada (1998), the IPA (the International Permafrost Association) established a Task Force on "Mapping and Distribution Modeling of Mountain Permafrost" (Hoelzle et al., 2001). The eighth International Conference on Permafrost in Zurich, Switzerland (2003) emphasized the study of the spatial permafrost models, in both arctic and high mountain environments. Since then, many models have been developed to predict the spatial variation of permafrost thermal response to changing climate conditions (Riseborough et al., 2008). The empirical-statistical model, which ignored the complicated energy exchange processes at the surface and within the active layer and related the permafrost presence directly with the BTS (Bottom Temperatures of Snow) values or the probability of permafrost occurrence to various influencing factors, is a common method in this art. Also the GIS technique, with its strong mapping and spatial analysis function and as an effective visualization tool of the permafrost distribution patterns, was used as well (Julián and Chueca, 2007; Heggem et al., 2005; Antoni et al., 2004; Gruber and Hoelzle , 2001; Etzelmüller et al., 2001). The BTS method, developed firstly in Haeberli's study of permafrost distribution in eastern Alps in 1973 and subsequently introduced into other mountainous area, had a strict boundary condition of a deep enough snow cover which could insulate the interface between the snow cover and ground surface from short variations of air temperatures. The drier continental climate in the mountains and high-altitude areas in China, which is characterized by small amounts of snow in winter, could not satisfy the boundary condition of BTS. In addition, the process-based models of permafrost, such as PERMABAL (Stocker et al., 2003) and PERMACLIM (Guglielmin et al., 2003), required a knowledge of the thermal exchange and energy balance process of permafrost.

For distribution patterns of the high-altitude permafrost in China, Cheng (1982) proposed the three-dimensional spatial features of vertical, latitudinal and aridity for the zoning of high-altitude permafrost distribution, as well as a draft classification of high-altitude permafrost according to the stability, indicated by its thickness and the mean annual ground temperature. In addition, the Gauss curve was used to fit the lower limit of high-altitude permafrost in Northern Hemisphere, which related the lower limit of high-altitude permafrost to the latitude. The validity of the curve based on data in Northern Hemisphere proved to be fairly good (Cheng and Wang, 1982; Cheng, 1984), and the curve used on the Qinghai-Tibetan Plateau also produced good results (Li and Cheng, 1999). Later, two statistical models based on the ground temperatures of high-altitude permafrost were constructed for modeling the distribution of permafrost along the Qinghai-Tibetan Highway and on the Qinghai-Tibetan Plateau, which took the latitude and altitude as dependent variables (Wu et al., 2000; Nan et al., 2002). The above models, which considered only the effects of the macro-factors of latitude and altitude on development of high-altitude permafrost, were appropriate on large scales. However, as the scale decreased, the effects of the local factors could not be ignored in the process of alpine permafrost development, and simply copying the above macro-scale models in meso- or micro- scales will necessarily lead to errors.

Therefore, this paper, taking the upper area of Shule River as the study area, aimed at studying the single effects of latitude, altitude, slope and aspect, as well as their combined effects on permafrost development indicated by ground temperature, on the basis of which a regional permafrost distribution model was developed and used to predict the distribution patterns of alpine permafrost. Finally, the calculated results were compared with that of the Gauss curve.

2 Study area

The Shule River basin is one of three inland river basins of the Gansu corridor in China, and the upper area of Shule River (96.6°~99.0° E 38.2°~40.0° N), which is located in

the western part of the Qilian Mountains, on the northeastern edge of the Qinghai-Tibetan Plateau, refers to that above the mountain-pass and has an area of appropriately 11348.35 km^2. Administratively, it extends across two counties of Tianjun and Subei, which, respectively belong to the Mongolian Autonomous Prefecture of Qinghai province and the Gansu province in western China (Fig. 1).Topographically, it consists of two mountain ranges, the southern Shule Mountains and the southern Tuolai Mountains with high altitudes and steep slopes, and the valley of the Shule River with lower altitudes and a gentler terrain (Fig. 2). Climatically, it is of the continental arid and desert type with low mean annual air temperatures and small amounts of yearly total precipitation. The values from two nearby meteorological stations of Tuole and Muli were −2.7° and 349.2 mm, −5.8° and 515.2 mm. The vegetation is of alpine meadow type with a degree of coverage ranged from 5% to 50% as obtained from TM remote sensing data, and is categorized as the middle and low coverage degree of vegetation cover.

3 Methodology

3.1 Borehole location and measurement of ground temperatures of permafrost

A field investigation was carried out at the beginning of May in 2008 to explore the general distribution pattern of permafrost along the valley of the Shule River, and the locations of borehole were determined primarily. Later, ten boreholes arranged mainly in the source valley of the River with their depths ranged from 8 to 15 m were drilled and the relative ground temperatures were measured. In detail, the purposes of the boreholes were (a) to determine the lower limit of permafrost in the source valley of the Shule River (BH_1, BH_2 and BH_3, which were defined as the lower limit boreholes of permafrost), (b) to analyze the impact of slope and aspect (BH_4, BH_5, $BH_6$and BH_7, these were defined as the micro-topographic boreholes), (c) to evaluate the effects of different surface conditions (BH_8, $BH_9$and BH_{10}, defined as the surface condition boreholes) on

HESSD
6, 5243–5278, 2009

the development of permafrost. The location of the boreholes with specific purposes is the basis of the study. Except for the two boreholes of BH_8 and BH_9 which were located specially for the comparison of the effects of different surface conditions on the development of permafrost, the other boreholes were arranged with a relatively uniform surface conditions – the vegetation was alpine meadow type with coverage c. 30 to 60%, the lithology of surface soil was sandy loam, and the water content of surface soil was 4 to 12%.

The shallow ground temperatures of permafrost at the depth of 0.5 m below the surface, the soil moisture at the depth of 0.05 m and the vegetation degree of coverage of the ground surface were measured using a thermistor probe, time domain reflectometry (TDR) of soil moisture and quadrats measurement during the measurements of ground temperatures at the borehole locations and some other places where the surface conditions were different from that of borehole points (Table 1). In this case, the ground temperatures of permafrost referred that of soil temperatures at the depth of 8 m below the surface and measured by a thermistor probe in the boreholes. A total of four measurements of data were obtained from the early of June to the end of November in 2008. The steadiest ground temperatures were used to analyze the influencing factors and construct a model to predict the distribution patterns of permafrost for the study area.

3.2 Terrain analysis

From the field investigation and measurements of soil wetness, it was found that the vegetation was sparse and the water content of surface soil was low. Therefore, it was thought that the topographic conditions were the main controlling factors for the distribution of permafrost in the study area. In addition, according to the classification principles of permafrost put forward by Zhou et al. (2000), the permafrost type distributed here is of the alpine permafrost zone in Altun-Qilian Mountains, the southwestern China geocryological area (Qinghai-Xizang Plateau). In this zone, altitude is the major factor governing the development of permafrost, and then latitude and longitude

are secondary factors. Therefore, the terrain analysis was made first of all.

As far as altitude is concerned, the range of elevation is between 2100–5750 m and the mean elevation is 3900 m. The regional DEM was divided into six altitude zones of lower than 3000 m, 3000–3500 m, 3500–4000 m, 4000–4500 m, 4500–5000 m, and 5000–5750 m with reference to the topographic situations. The lowest altitude zone of lower than 3000 m is located at the mountain-pass valley of the Shule River; it was therefore named as the mountain-pass valley. Similarly, the other five altitude zones were, respectively named as the middle valley, the source valley and the front edge area of two mountains, the low mountainous area, the middle mountainous area and the high mountainous area according to the topographical characteristics of their locations. The area percentages of each altitude zone accounting for the total area were 7, 11, 33, 35, 12 and 2, respectively. Therefore, 3500–4000 m and 4000–4500 m are the two major altitude zones, that is to say, the source valley and the front edge area of two mountains, as well as the low mountainous area are the major terrain types (Table 2). In addition, glaciers are distributed in the highest altitude zone of 5000–5750 m.

3.3 Topo-climatic factors

The location of each borehole was recorded using a handheld Global Position System (GPS) (Garmin E-trex Summit 12XL) in WGS 84 coordinates. The topographic factors of elevation, slope, aspect and shade were computed using the surface analysis procedure of the GIS software with 50 m-DEM data from the Environmental and Ecological Science Data Center for West China.

The calculation of solar radiation for the whole study area and each borehole site was carried out using the Solar Analyst program within the software of ESRI's ArcView 3.2. It could calculate three solar radiation variables of the potential direct, diffuse and global incoming radiation for any time period and spatial extent. The total potential direct incoming radiation in a year was chosen to analyze the relationship between solar radiation and ground temperatures of permafrost. The Solar Analyst program is a topographic radiation balance model suitable for the calculation of the potential incoming

HESSD
6, 5243–5278, 2009

solar radiation under the complex topographic situations (Heggem et al., 2001). It takes into account site latitude and elevation, slope, surface orientation, shadows cast by surrounding topography, daily and seasonal shifts in solar angle, and atmospheric attenuation. The surface albedo is not included in the model (Fu and Rich, 2000).

4 Models

4.1 Determination of the lower limit of permafrost in the source valley of Shule River

In the field investigation, the lower limit of permafrost in the source valley of the Shule River was determined at the height of *c*. 3700 m on the shady slope and *c*. 3800 m on the sunny slope. Then, the measurement of ground temperatures in the three boreholes of BH_1, BH_2 and BH_3 proved that these three boreholes were located in the transition zone between perennially frozen ground and seasonally frozen ground. Based on the borehole core data and the ground temperature curves of the three boreholes, the lower limit of permafrost in the source valley was finally determined at an altitude of 3727–3750 m (Fig. 3). In order to quantify the effects of the influencing factors on the development of permafrost and construct a corresponding mathematic model, the altitude of BH_1 was defined as the lower limit of permafrost in the source valley and its ground temperatures as 0°.

4.2 Calculation of equivalent-elevation and construction of a ground temperatures – equivalent elevation equation

Taking the four boreholes of BH_1, BH_2, BH_3 and BH_{10}, which were located in the same flat valley of Shule River but with different altitudes and latitudes, as the analysis objects, the influence of latitude and altitude on development of permafrost were evaluated and analyzed.

According to the Gauss curve proposed by Cheng (1982), it is known that the altitude of permafrost lower limit in Northern Hemisphere does not increase monotonously, but first increases starting from the equator with increasing latitude and reaches its maximum value of 5078 m at the latitude of 25°22′ N, and then decreases with increasing latitude. Initially, the slope of the decrease gets steeper, and is steepest at latitude of 38° N, then flattens off with increasing latitude. The upper area investigated just lies in the region with the steepest slope of the Gauss curve, and a small variation of geographic latitude will lead to a corresponding large variation in the lower limit of permafrost. This was proved by the results calculated for the four boreholes with the Gauss curve (Table 3). Therefore, the following conclusions can be concluded. First of all, the effects of latitude on the development of permafrost in this area should not be ignored even though it has a small spatial extent. Secondly, the effects of elevation in the study area actually reflect the double influence of elevation and latitude on ground temperatures of permafrost. On the basis of these conclusions, the concept of Equivalent-elevations was introduced and the effect of latitude on development of permafrost was embodied in the form of an altitudinal difference.

The computation of equivalent-elevations involves three steps. First of all, the lower limit of every point is calculated based on the Gauss curve. Then, the altitudinal differences of the lower limits are calculated by determining a datum mark. Finally, the altitudinal differences of the lower limits from the latitudes are added to the actual altitude and the relative equivalent-elevation of every point is obtained.

The equivalent-elevation values of the four boreholes were calculated with reference of the BH_{10} (Table 3), and a good linear relationship was found between them and their ground temperature values (Fig. 4).

On the basis of the calculation of the equivalent-elevation values and the good linear relationship between the equivalent-elevation values and ground temperatures of the four boreholes, a Ground Temperature – Equivalent Elevation Equation (GT-EE Equation) was developed to calculate the effects of latitude and altitude on the distribution of permafrost.

4.3 Calculation of potential direct solar radiation and construction of a radiation adjustment equation

In the mountainous area, the complex terrain conditions have two effects on the development of permafrost. One is the aspect-depending radiation effects and the other is changes of air temperature with altitude and topographic-caused snow influences (Etzelmüller et al., 2001). With the increase in altitude, the air temperature decreases and forms a cold climate background contributing to the development of permafrost. The influence of slope, aspect and shade on the amount of incoming to the surface solar radiation greatly over short distances. Especially in steep topographic areas, as well as on sunny and shady slopes, this kind of spatial change of solar radiation is quite prominent and affects directly the development of permafrost at some points.

However, previous quantitative evaluations about the influence of solar radiation on ground temperature of permafrost are few. Several empirical-statistical models' results based on BTS measurements indicate that there exists a linear relationship between BTS values and elevation, BTS and the incoming solar radiation (Gruber and Hoelzle, 2001; Antoni et al., 2004; Julián and Chueca, 2007). In addition, a good linear relationship was found between shallow ground temperature (0.5 m) and the potential incoming solar radiation on the slope of the roadbed in the Beiluhe area on the Qinghai-Tibetan Plateau in China (Chou et al., 2008). Therefore, the assumption that there is a linear relationship between ground temperature and the incoming solar radiation is the basis of next analysis and was validated by the measurements.

Four boreholes BH_4, BH_5, BH_6 and BH_7 located on different slopes and aspects with the special purpose of evaluating the effect of the micro- topographic factors on ground temperatures of permafrost were chosen and the relative potential direct solar radiation (PDSR) was calculated. In the process of the calculations, in order to avoid the influence resulting from the random borehole locations, the point-based calculation of PDSR using a specific slope and aspect was substituted with a range of slope and aspect values. The resultant PDSRs were also range values, and the maximum of the

range values was defined as the model-based PDSR at the four locations (Table 4).

Comparing ground temperatures of permafrost at the four points with the PDSRs, a significant positive correlation was discovered, at the same time a linear relationship between the increments of PDSR and ground temperature was found. As the ground temperatures changed by 1°, the gradient of PDSR varied by approximately 500 kWh/m^{2}·°. Accordingly, a Radiation Adjustment Equation (RA Equation) was constructed based on the calculation of PDSR and the determination of the gradient of PDSR.

4.4 Development of a regional permafrost distribution model (RPD Model)

Finally, a regional permafrost distribution model (RPD Model), based on the two equations, the GT-EE Equation and the RA Equation, was developed and the ground temperatures of permafrost were calculated. Based on the model the individual effect of latitude, altitude, slope and aspect, and the combined effects of these factors on the development of permafrost could be quantitatively evaluated.

The expression of the RPD Model is as follows:

$$GT = GT_{h'} + \Delta GT_s$$

in which, the expressions of the GT-EE Equation and the RA Equation are, respectively $GT_{h'} = -0.0038^{*}h' + 14.317$ and $\Delta GT_s = (R - R_0)/500$

Where GT is the ground temperature of permafrost predicted by the RPD Model (°), $GT_{h'}$ is the ground temperature of permafrost determined by the GT-EE Equation, which shows the effects of latitude and altitude on the development of permafrost (°). ΔGT_s is the increment of ground temperature relative to a datum mark and calculated using the RA Equation (°), h' is the equivalent-elevation (m). R is the PDSR at a specific point (kWh/m^{2}) and R_0 is the datum mark of PDSR, which refers to that of the lower limit of permafrost in the source valley (kWh/m^{2}).

The ground temperature of 0° is the critical value of perennially frozen ground and seasonally frozen ground. Furthermore, a classification principle of permafrost

based on the ground temperatures was adopted and the permafrost was divided into four types: low-temperature permafrost (GT≤−2°), middle-temperature permafrost (−2°<GT ≤−1°), high-temperature permafrost (−1°<GT ≤−0.5°) and extreme high-temperature permafrost (−0.5°<GT ≤0°) (Wu Ziwang and Liu Yongzhi, 2005).

5 Results

5.1 Distribution patterns of permafrost

The frozen ground map, as well as the classification map of permafrost of this area was constructed using the RPD Model within the ARCGIS software (Fig. 5). Zonal statistics, a GIS overlay method, were processed using four pairs of raster data: DEM and reclassified frozen ground, DEM and reclassified permafrost, reclassified DEM and reclassified frozen ground, reclassified DEM and reclassified permafrost successively. The spatial distribution patterns of perennially frozen ground and seasonally frozen ground, as well as all permafrost types were obtained using this procedure.

The results showed that 83% of the upper area was underlain by perennially frozen ground and the distribution area was 9447.16 km^2. The rest area of 1901.19 km^2 was underlain the seasonally frozen ground and accounted for 17%. For the permafrost, the low-temperature permafrost was the main permafrost type, and its distribution area and percentage were 4352.90 km^2 and 38%. Next was the middle-temperature permafrost with an area and percentage of 2603.53 km^2 and 23%. The areas and percentages of high-temperature and extreme high-temperature permafrost were comparatively small and the values were 1625.20 km^2 and 14% for the high-temperature permafrost, and 865.53 km^2 and 8% for the extreme high-temperature permafrost, respectively.

Topographically, the low-temperature permafrost was distributed widely in the high, middle, lower mountainous area and the front edge of two Mountains, as well as the source and middle valley of the Shule River covering the altitude range of 3000 m to 5750 m, i.e. except for the lower-altitude area of mountain-pass valley, all the other

areas were more or less underlain with the low-temperature permafrost. And the distribution percent of low-temperature permafrost in each altitude zone were 5% (5000–5750 m), 32% (4500–5000 m), 56% (4000–4500 m), 7% (3500–4000 m). Thus, it can be concluded that the middle and lower mountainous area were the main areas of distribution. The middle-temperature permafrost was distributed in the low mountainous area, the front edge areas, the source valley and the middle valley. The distribution pattern is 54% within the altitude zone of 4000 m to 4500 m, 45% in the zone 3500 m to 4000 m and only 1% in the zone 3000 m to 3500. Therefore, it is clear that the areas of lower mountainous areas, the front edge area and the source valley were the main distribution areas of the middle-temperature permafrost. The high-temperature permafrost type was spatially widespread and the low mountains, the front edge area and all the valley of the River were underlain by this kind of permafrost where the altitude ranged from 2100 m to 4500 m, in which the front edge area and the source valley (3500–4000 m) were the main areas of distribution of this kind of permafrost with 91% in this zone. The extreme high-temperature permafrost was distributed in the altitude zones 3500–4000 m and 3000–3500 m with 67% and 33%, respectively, see (Fig. 6).

5.2 Effects of micro-topography on the distribution of permafrost

The prediction results of the RPD Model were obtained by adding the calculated results of the RA Equation to those of the GT-EE Equation. The calculated results of the GT-EE Equation were not adjusted by the solar radiation, yet the prediction results of the RPD Model were. Therefore, both the results of the GT-EE Equation and the RPD Model were compared to find the differences in extent and places of ground temperature of permafrost to evaluate quantitatively the effects of the micro-topographic factors slope and aspect on the development of permafrost. Some conclusions were obtained from this comparison.

After adjustment, the total distribution area of permafrost increased by 766.22 km^2 which is 8% of all the permafrost area. It can be argued that the effects of micro-topography account for 8% of the permafrost and the other 92% result from altitude and latitude. In the area above the lower limit of permafrost, which accounts for nearly 80%, the adjustment of solar radiation can only change the ground temperatures of permafrost but not change the permafrost type; therefore, altitude is the major controlling factor for permafrost development. Topographically, the increase of permafrost area mainly occurred in the two altitude zones of 3000–3500 m and 3500–4000 m, and was 390.72 km^2 and 375.45 km^2, respectively, see (Fig. 7). These are the altitude zones of lower and around the lower limit of permafrost. The increase of permafrost in these areas shows the effects of micro-topography on the development of permafrost, i.e. the effects of micro-topography caused the development of permafrost in local lower-altitude areas.

After the adjustment for solar radiation, the areas of low- and middle-temperature permafrost increased, and the high- and extreme high- temperature permafrost decreased (Fig. 8). In fact, the low-temperature permafrost distributed in the middle and high mountainous areas did not experience any change, and the increase in area occurred mainly in the low mountainous area (620.04 km^2), the front edge area and the source valley (315.56 km^2), which increased the area of low-temperature permafrost by 935.60 km^2. The area of middle-temperature permafrost decreased by 612.81 km^2 in the low mountainous area, but increased by 589.34 km^2 and 28.18 km^2 in the source valley and the front edge area, which increased the total area of the middle-temperature permafrost by small amount of 4.71 km^2. At the same time, an increase of the high-temperature permafrost type of 75.61 km^2 occurred mainly in the middle valley area, but it decreased 7.23 km^2 and 113.48 km^2 in the low mountainous area, the front edge and the source valley, therefore, the area of the high-temperature permafrost decreased by a total of 45.09 km^2 after the adjustment. Similarly, the area of the extreme high-temperature permafrost increased by 286.89 km^2 in the middle valley, and decreased by 415.98 km^2 in the source valley and the front edge, thus the area of the

HESSD
6, 5243–5278, 2009

high-temperature permafrost decreased by 129.05 km^2 after the adjustment (Fig. 9).

The change in area after adjustment with the SA equation was largest for the low-temperature permafrost, followed by the extreme high-temperature permafrost.

5.3 Analysis of change in ground temperature caused by the radiation adjustment equation

Comparing the calculated results of ground temperature of the GT-EE Equation and the RPD Model, there was no ground temperature change in 54% of the area, the ground temperature decreased by 1° in 43% of the area, a decrease of 2° occurred in 3% of the area. There was a small area where the ground temperature increased. Therefore, ground temperatures of no change or decreasing by 1° were the main changes after the adjustment.

The percentages of the area with ground temperature decreasing by 1° was 1% in the high mountainous area, 11% in the middle mountainous area, 25% in the low mountainous area, 28% in the front edge area and the source valley, 20% in the middle valley and 14% in the mountain-pass valley. Therefore, the main changes occurred in such areas as the low mountainous area, the front edge, the source valley and the middle valley at altitudes between 3000 m to 4500 m. In addition, 6% of the area with ground temperature decreasing by 1° was located on flat areas, 42% occurred on the shady slopes with a 0–90° aspect, 7% occurred on the sunny slopes with a 90–180° aspect, 10% occurred on the sunny slopes with a 180–270° aspect, and 35% occurred on the shady slope with a 270–360° aspect. More than three quarters of the area where the ground temperature decreased by 1° were distributed in the shady slope, which proved the great effect of slope and aspect on the development of permafrost.

5.4 Comparison of the results between the RPD model and the Gauss curve

Based on the Gauss curve proposed by Cheng (1982), the upper area was divided into two types, one was underlain by perennially frozen ground and the other was

HESSD
6, 5243–5278, 2009

seasonally frozen ground. The permafrost map predicted by the Gauss curve was prepared using the ARCGIS software and the resultant map was compared visually with that of the RPD Model (Fig. 10).

The results of the Gauss curve showed that the distribution area of the perennially frozen ground was 9380.50 km^2 corresponding to 83% in the total area and the area of the seasonally frozen ground was 1967.85 km^2 corresponding to 17%.

A comparison of the two results indicated an approximately equal area of permafrost. However, for the spatial distribution patterns of permafrost, especially in the low altitude zone of 3000–3500 m, the two results were significantly different from each other. The results of the Gauss curve showed that an area of 106.25 km^2 is underlain by permafrost in this altitude zone which accounts for 1% of the whole area, whereas the results of the RPD Model showed that the area of 390.72 km^2 is underlain by permafrost in the same altitude zone which accounts for 4% of the study area (Fig. 11). The difference in the two results lay in the fact that the topo-climatic factors of latitude, elevation, slope and aspect were all considered in the RPD Model, but only the macro-scale factors of latitude and elevation were considered in the Gauss curve. In the mountainous area with complicated terrain conditions, the micro-topographic factors of slope and aspect have a large effect on the spatial distribution situations of the incoming solar radiation. At some local lower-altitude areas, the influence of slope and aspect caused the incoming solar radiation reaching the ground surface to decrease and permafrost developed, which has been shown in this study.

The results calculated from the Gauss curve showed that the lowest altitude of lower limit of permafrost was at a height of 3385 m. However, the field investigation and measurements showed that the lower limit of permafrost in the source valley lay between 3727 m to 3750 m. Accordingly, the Gauss curve increased the extent of permafrost in the altitude zone of 3500–4000 m, and made the modeling area of permafrost (3725.25 km^2) a little larger than that of the RPD Model in this zone (3544.40 km^2).

Both results indicate that the altitude zones of 3500–4000 m, 4000–4500 m and 4500–5000 m are the major altitude zones of permafrost distribution in this area, and

the percentages in these three altitude zones were, respectively 38, 42, 15 (the Gauss curve) and 40, 42, 15 (the RPD Model). Therefore, topographically, the middle and low mountainous area, the front edge and the source valley were the major distribution regions of permafrost. The reasons for the distribution of the patterns of permafrost involved twp factors. One was that the altitude is the main factor determining the distribution patterns of permafrost above the height of 3500 m. The micro-factors of slope and aspect only change the local distribution patterns. The other is that the altitude of 3500 m to 5000 m is the major altitude zone in the upper area and accounts for 80% in the area.

6 Conclusion and discussion

The popular empirical-statistical models, which relate the BTS values or probabilities of permafrost occurrence to altitude and incoming solar radiation, can predict the existence probabilities of permafrost (Julián and Chueca, 2007; Heggem et al., 2005; Antoni et al., 2004; Gruber and Hoelzle 2001; Etzelmüller et al., 2001). In China, the effects of latitude and altitude on the development and distribution of permafrost have been studied in detail (Cheng and Wang, 1982; Cheng, 1984; Wu et al., 2000; Nan et al., 2002), but quantitative studies on the effects of micro-topographical factors of slope and aspect were not carried out until now.

This research, based on the field investigation and combined with the measurement of ground temperature, tried to evaluate quantitatively the single effect of latitude, altitude, slope and aspect, as well as their combined effects on permafrost development by developing the GT-EE Equation, the SA Equation and the RPD model. Some conclusions were obtained, but there still some open questions.

Due to problems of accessibility of drilling machines and economic reasons, the location and number of boreholes were greatly restricted. The ten boreholes were mainly located in the flat source valley. The fact that the number of borehole was small and only located in the flat area made the representation of sampling poor, and

made the validity of the prediction results impossible. However, the specific purposes of boreholes arrangement provided the stable data basis for this study. Therefore, it is necessary to increase the number of boreholes and extend the spatial distribution of the boreholes in a further study.

For the construction of the GT-EE Equation and the SA Equation which were used to depict the relationship between ground temperature and the macro-factors of latitude and altitude, as well as the relationship between ground temperature and the micro-topographic factors of slope and aspect, it is necessary to assume other factors, such as vegetation, lithology and soil wetness, are relatively uniform. In this case, however, due to lack of accurate values of the other factors, the uniform condition had to be verified by field observations, which maybe have resulted in some uncertainties. Therefore, more exact values should be obtained in future studies.

The distribution of alpine permafrost is a complicated phenomenon because many factors have their respective effects on the development of permafrost in alpine environments, and there exists complex interactions between these factors. It is therefore very difficult to make a quantitative evaluation of a single factor's effect on the development and distribution of permafrost. In this study, the effects of latitude, altitude, slope and aspect were considered and a quantitative evaluation was attempted, but more local factors should be studied further in the future.

The following conclusions were obtained from this study.

From the analysis of the factors, it was discovered that the altitude was the major factor controlling the distribution of permafrost in the upper area. This directly determined the macro-scale distribution patterns of frozen ground. And the effect of latitude on the distribution of permafrost could not be ignored even on the drainage basin scale. The influence of solar radiation on the spatial distribution patterns of permafrost was small and focused on the local shade areas at lower altitudes.

The results of the RPD model indicated that the area of permafrost was 9447.16 km^2 and accounted for 83% of the total area. At the same time, the classification of permafrost was carried out based on ground temperatures and the distribution patterns

HESSD
6, 5243–5278, 2009

of all types of permafrost were analyzed as well. The low-temperature permafrost (GT≤-2°) was the major type and accounted for 38% of the total area, which was distributed mainly in the middle and lower mountainous areas at altitude zones of 4500–5000 m and 4000–4500 m. The middle-temperature permafrost (−2°<GT ≤−1°) was the second largest type in the area and accounted for 23% of the total area, which was distributed mainly in the lower mountainous areas, the front edge and the source valley with altitude zones of 4000–4500 m and 3500–4000 m. The percentages of high-(−1°<GT ≤−0.5°) and extreme high-temperature permafrost (−0.5°<GT ≤0°) were small and the values were 14% and 8%, respectively, and were distributed in the front edge and the source valley in the altitude zone of 3500–4000 m.

In addition, the adjustment of solar radiation with the SA Equation proved that altitude zone of 3500–4000 m, as well as the shady slopes in different altitude zones were the most obvious areas of changes in ground temperature of permafrost resulting from the micro-topographic factors of slope and aspect. The comparison of the two results from the RPD model and the Gauss curve showed that in both cases the distribution area of permafrost was approximately the same. However, the spatial distribution patterns of permafrost, especially in the low altitude zone of 3000–3500 m, the results of the RPD model were much larger than those from the Gauss curve. This is because the effects of local topographical factors of slope and aspect on the distribution of permafrost were considered in the RPD model but not in the Gauss curve.

Acknowledgements. This research was supported financially by the National Basic Research Program of China (973 Program, grant no. 2007CB411502) and the National Science Foundation of China (grant no. 40871040). The field investigation was carried out by the State Key Laboratory of Frozen Soil Engineering and State Key Laboratory of Cryospheric Science, Cold and Arid Regions Environmental and Engineering Research Institute, Chinese Academy of Sciences. Thanks to the Environmental and Ecological Science Data Center for West China (http://westdc.westgis.ac.cn/), the 50 m-DEM data of the area was offered by the Data Center.

References

Cheng G. and Wang S: On the zonation of high-altitude permafrost in China, Journal of Glaciology and Geocryology, 4, 1–16, 1982.

Cheng, G: Problems on zonation of high-altitude permafrost, J. Geogr. Sci., 39, 185–193, 1984.

Chou, Y., Sheng, Y., Ma, W., and Li, J.: Discussion on shallow ground temperature of embankment in permafrost regions on the Qinghai-Tibet Plateau, Soil Engineering and Foundation, 22, 44–48, 2008.

Etzelmüller, B., Hoelzle, M., Heggem, E.S.F., Isaksen, K., and Mittaz, C.: Mapping and modelling the occurrence and distribution of mountain permafrost, Norw. J. Geol., 55, 186–194, 2001.

Etzelmüller, B., Heggem, E. S. F., Sharkhuu, N., and Frauenfelder, R.: Mountain permafrost distribution modelling using a multi-criteria approach in the Hövsgöl Area, Northern Mongolian, Permafrost Periglac., 17, 91–104, doi:10.1002/ppp.554, 2006.

Fu, P. and Rich, P. M.: Design and implementation of the Solar Analyst: an ArcView extension for modeling solar radiation at landscape scales, http://gis.esri.com/library/userconf/proc99/proceed/papers/pap867/p867.htm, access: 15 October 2007.

Gruber, S. and Hoelzle, M.: Statistical modelling of mountain permafrost distribution – local calibration and incorporation of remotely sensed data, Permafrost Periglac., 12, 69–77, doi:10.1002/ppp374, 2001.

Guglielmin, M., Aldighieri, B., and Testa, B.: PERMACLIM: a model for the distribution of mountain permafrost, based on climatic observations, Geomorphology, 51, 245–257, doi:10.1016/S0169-555X(02)00221-0, 2003.

Heggem, E. S. F., Etzemüller, B., and Berthling, I.: Topographic radiation balance models: sensitivity and application in periglacial geomorphology, Norw. J. Geol., 55, 23–28, doi:10.1002/ppp384, 2001.

Heggem, E. S. F., Juliussen, H., and Etzemüller, B.: Mountain permafrost in Central-Eastern Norway, Norw. J. Geol., 59, 94–108, doi:10.1080/00291950510038377, 2005.

Hoelzle, M., Mittaz, C., Etzemüller, B., and Haebweli, W.: Surface energy fluxes and distribution models of permafrost in European mountain areas: an overview of current developments, Permafrost Periglac., 12, 53–68, doi:10.1002/ppp385, 2001.

Jin, H., Zhao, L., Wang, S., and Jin, R.: The characteristics of ground temperatures and the degradation styles of permafrost along the Qinghai-Tibet highway, Sci. China Ser. D, 36,

1009–1019, 2006.
Julián, A. and Chueca, J.: Permafrost distribution from BTS measurements (Sierra de Telera, Central Pyrenees, Spain): assessing the importance of solar radiation in a mid-elevation shaded mountainous area, Permafrost Periglac., 18, 137–149, doi:10.1002/ppp.576, 2007.
Lewkowicz, A. G. and Ednie, M.: Probability mapping of mountain permafrost using the BTS method, Wolf Creek, Yukon Territory, Canada, Permafrost Periglac., 15, 67–80, doi:10.1002/ppp.480, 2004.
Li, X. and Cheng, G.: The response model of high-altitude permafrost to global climate change, Sci. China Ser. D, 29, 185–192, 1999.
Nan, Z., Li, S., and Liu, Y.: Mean annual ground temperature distribution on the Tibetan Plateau permafrost distribution mapping and further application, Journal of Glaciology and Geocryology, 24, 142–148, 2002.
Riseborough, D., Shiklomanov, N., Etzelmüller, B., Gruber, S., and Marchenko, S.: Recent Advances in Permafrost Modelling, Permafrost Periglac., 19, 137–156, doi:10.1002/ppp.615, 2008.
Stocker, M., Hoelzle, M., and Haeberli, W.: Modelling alpine permafrost distribution based on energy-balance data: a first step, Permafrost Periglac., 13, 271–282, doi:10.1002/ppp.426, 2002.
Wu, Q., Li, X., and Li, W.: Computer simulation and mapping of the regional distribution of permafrost along the Qinghai-Xizang Highway, Journal of Glaciology and Geocryology, 22, 323–326, 2000.
Wu, Z. and Liu, Y. : Frozen Subsoil and Engineering, Ocean Press, Beijing, China, 124–134, 2005.
Zhou, Y., Qiu, G., Guo, D., Cheng, G., and Li, S.: Frozen ground in China, Science Press, Beijing, China, 309–310, 2000.

Table 1. Boreholes information in the upper area of the Shule River.

ID	Ele.	Veg. Cov.	Soi. Moi.	GTs	Terrain interpretation of boreholes
BH_1	3727	30	6.77	0.7	A borehole of the lower limit at the source valley of the River
BH_2	3800	35	3.53	−40.2	A borehole to determine the lower limit of permafrost at the source valley of the River
BH_3	3825	50	9.38	−0.4	A borehole to determine the lower limit of permafrost at the source valley of the River
BH_4	3845	40	8.55	−0.4	A borehole located at the foot of a sunny slope
BH_5	3854	50	4.05	0.2	A borehole located on a sunny slope
BH_6	3860	50	3.73	0	A borehole located on a sunny slope
BH_7	3854	50	11.69	−0.8	A borehole located on a shady slope
BH_8	3895	80	7.18	−0.2	A borehole used to compare the different surface conditions
BH_9	3899	60	6.74	−0.1	A borehole used to compare the different surface conditions
BH_{10}	3900	30	5.55	−0.5	A borehole used to compare the different surface conditions

In the table, Ele. is elevation (m); Veg. Cov. is vegetation cover (%); Soi. Moi. is soil moisture (%); GTs is the ground temperatures in the boreholes at a depth of 8 m below the surface (˚).

HESSD
6, 5243–5278, 2009

Table 2. The topographic characteristics of the study area.

Altitude zone (m)	Area (km^2)	Percentage (%)	Mean slope (°)	Terrain features
2100–3000	772.55	7	9.84	The mountain-pass valley
3000–3500	1308.93	11	14.32	The middle valley
3500–4000	3739.38	33	10.62	The source valley and the front edge area
4000–4500	3935.27	35	12.69	The low mountainous area
4500–5000	1386.84	12	18.97	The middle mountainous area
5000–5750	205.39	2	20.50	The high mountainous area

HESSD
6, 5243–5278, 2009

Table 3. The variation of lower limits with latitudes and calculation of equivalent-elevations for the four boreholes with the Gauss curve.

ID	Ele. (°)	Lat. (m)	Lower limit (m)	Latitudinal difference (°)	Altitudinal difference (m)	Equivalent -elevation (m)
BH_1	38.6344	3727	3581	0.21	−37	3764
BH_2	38.5682	3800	3592	0.15	−25	3825
BH_3	38.5512	3825	3595	0.13	−22	3847
BH_{10}	38.4211	3900	3618	0	0	3900

In the table, Lat. and Ele. are the abbreviations of latitude and elevation. Lower limit referred to the calculated lower limits of the four boreholes based on the Gauss curve. Latitudinal difference and Altitudinal difference referred to difference values between lower limits with reference to BH_{10}.

HESSD

6, 5243–5278, 2009

Table 4. The calculated PDSR of boreholes located at different terrain conditions.

		Range of slopes	Range of aspects	Range of PDSRs
ID	Location of boreholes	(°)	(°)	(kWh /m^2)
BH_4	At the foot of a sunny slope	2–4	160–200	1452–1616
BH_5, BH_6	On a sunny slope	16–18	160–200	1616–1820
BH_7	On a shady slope	16–18	340–20	842–1283

HESSD

6, 5243–5278, 2009

Fig. 1. Location of the study area.

HESSD
6, 5243–5278, 2009

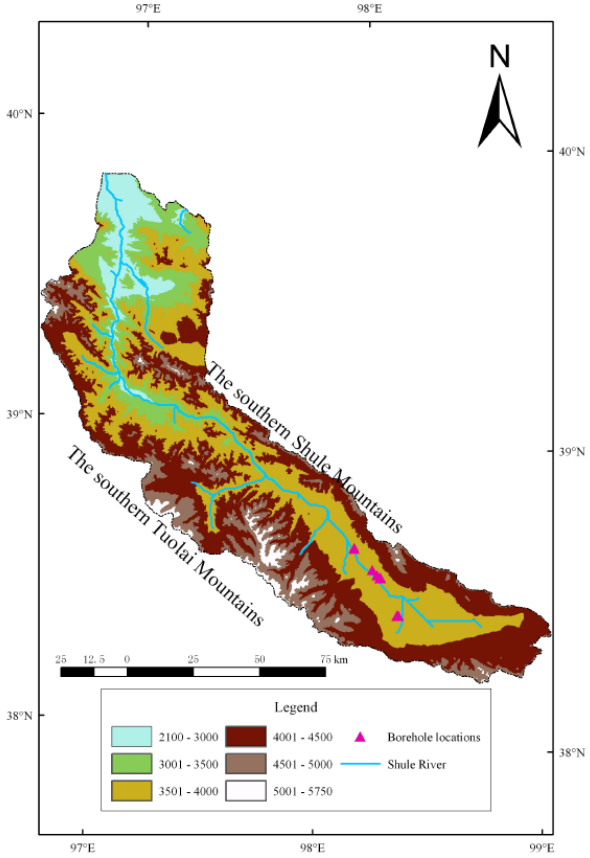

Fig. 2. DEM of the study area and the location of the boreholes.

HESSD
6, 5243–5278, 2009

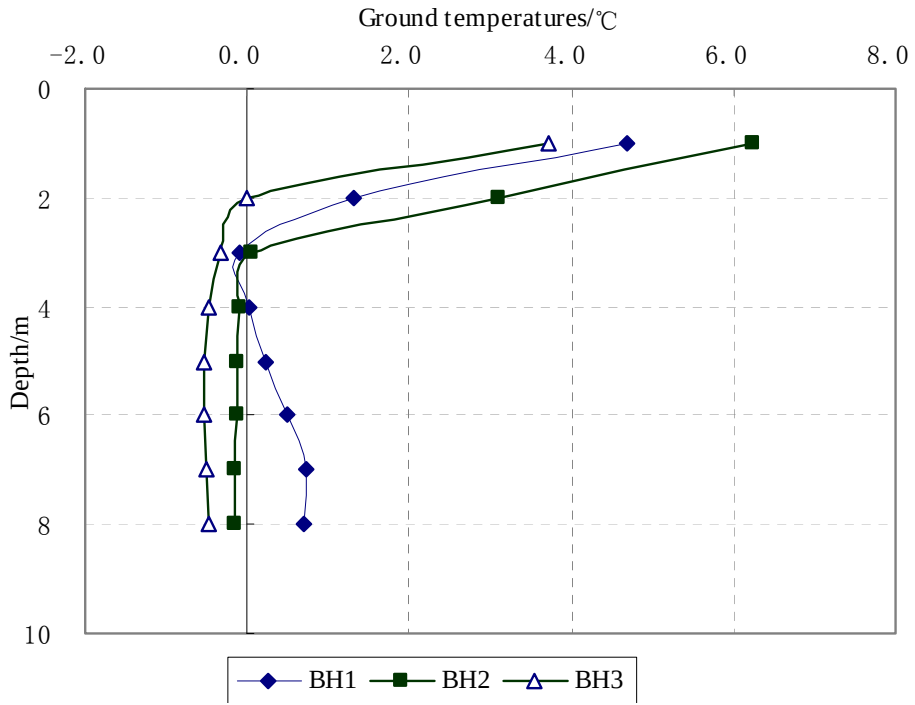

Fig. 3. Ground temperature curves of BH1, BH2 and BH3.

HESSD
6, 5243–5278, 2009

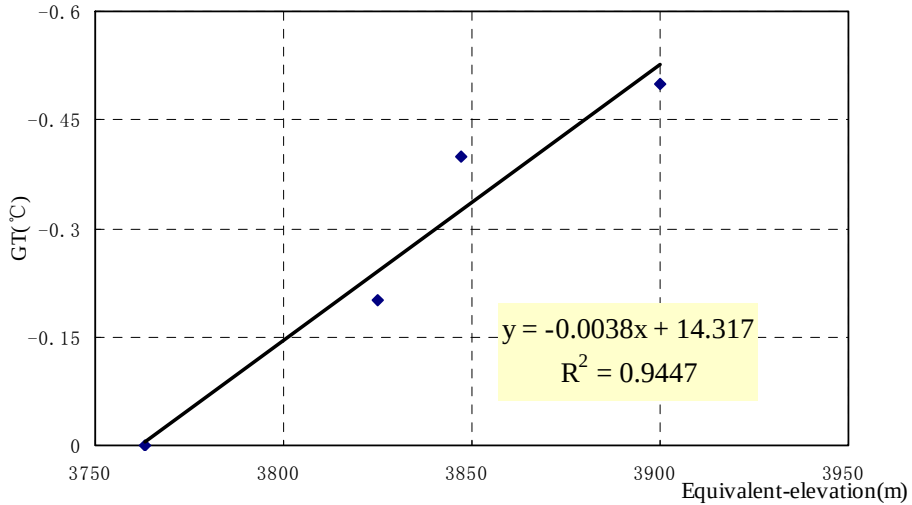

Fig. 4. The linear relationship between ground temperatures and equivalent-elevations at the four borehole points.

HESSD
6, 5243–5278, 2009

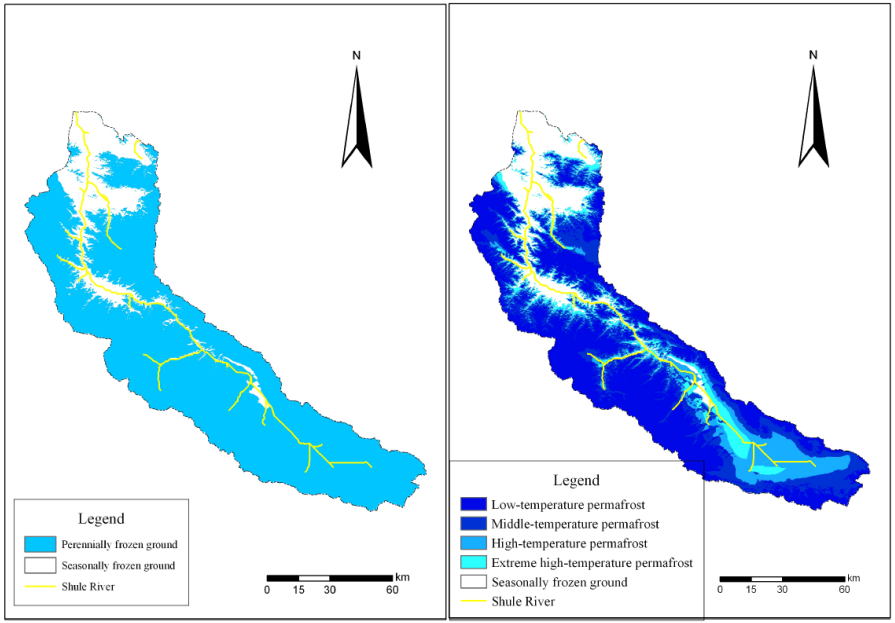

Fig. 5. The permafrost distribution map of the upper area predicted by the Regional Permafrost Distribution Model.

HESSD
6, 5243–5278, 2009

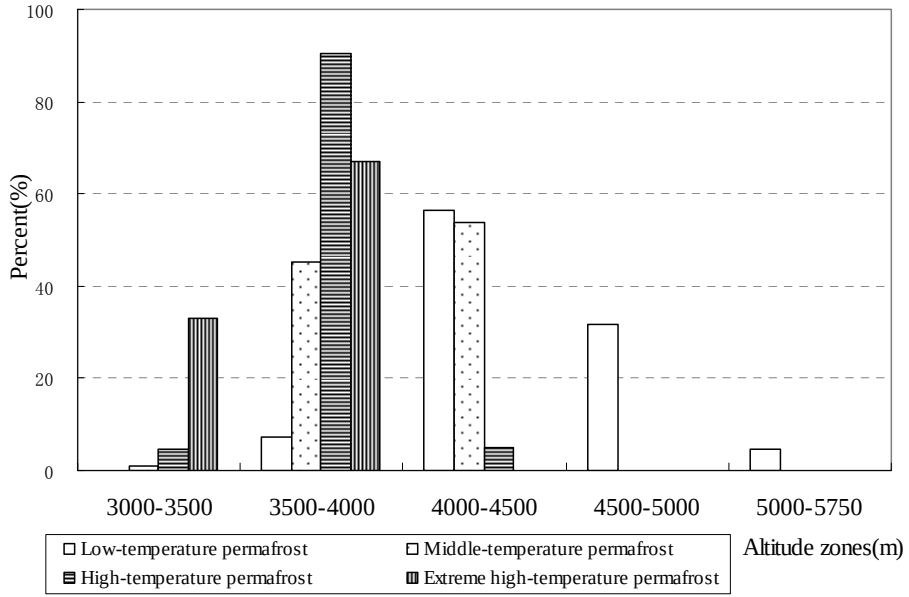

Fig. 6. The distribution patterns of all permafrost types in different altitudinal zones.

HESSD
6, 5243–5278, 2009

A regional model to predict the distribution of alpine permafrost

Y. Sheng et al.

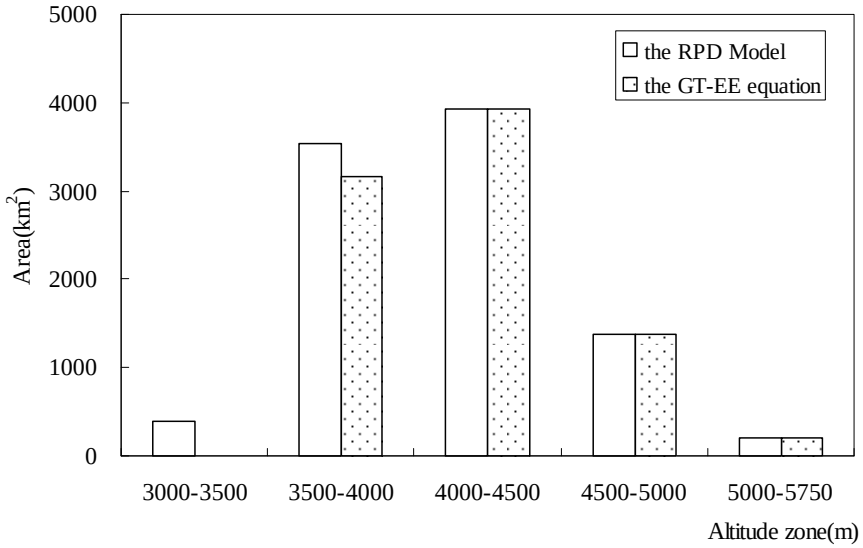

Fig. 7. Comparison of permafrost areas before and after adjustment of solar radiation.

HESSD
6, 5243–5278, 2009

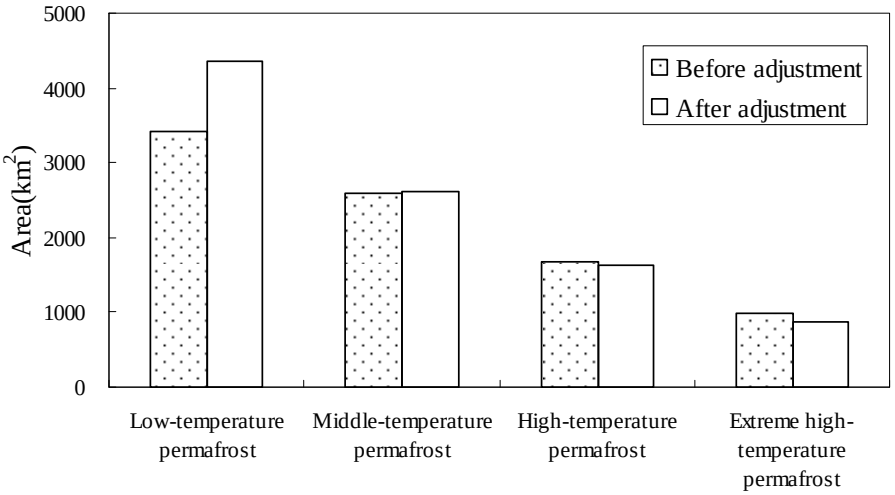

Fig. 8. Comparison of the distribution areas of all types of permafrost before and after adjustment of solar radiation.

HESSD
6, 5243–5278, 2009

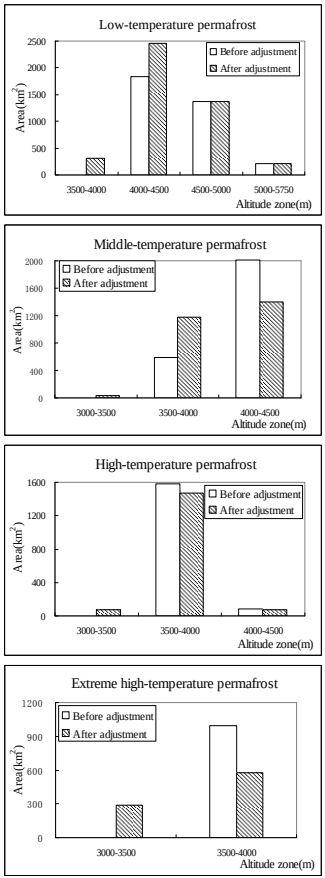

Fig. 9. Variation of distribution patterns of every permafrost type before and after adjustment of the solar radiation.

HESSD
6, 5243–5278, 2009

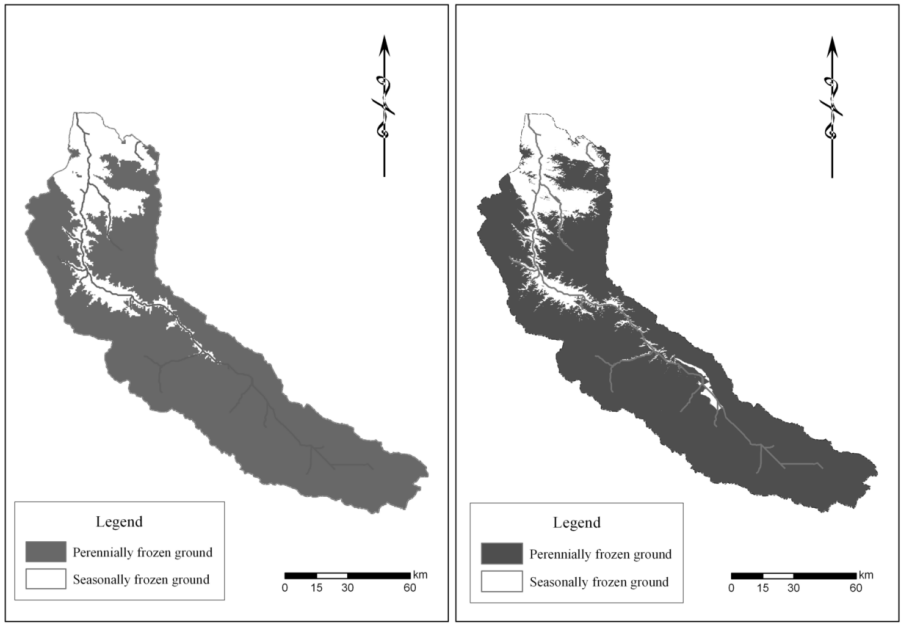

Fig. 10. The permafrost distribution maps based on the Gauss curve (on the left) and the RPD Model (on the right).

HESSD
6, 5243–5278, 2009

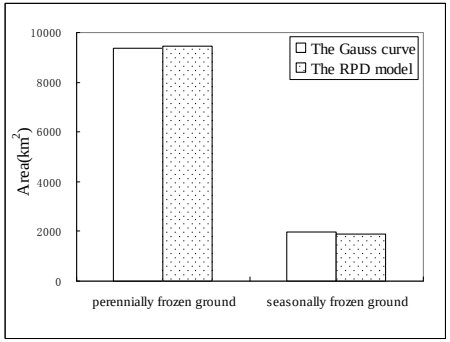

Fig. 11. Comparison of two results of the Gauss curve and the RPD Model.

HESSD
6, 5243–5278, 2009